IEEE Access
Multidisciplinary | Rapid Review | Open Access Journal

Received March 9, 2017, accepted March 22, 2017, date of publication April 3, 2017, date of current version June 28, 2017.

Digital Object Identifier 10.1109/ACCESS.2017.2690407

First Steps Towards Translating HZD Control of Bipedal Robots to Decentralized Control of Exoskeletons

AYUSH AGRAWAL[1], OMAR HARIB[2], AYONGA HEREID[2], SYLVAIN FINET[4,5], MATTHIEU MASSELIN[4], LAURENT PRALY[6], AARON D. AMES[3], KOUSHIL SREENATH[1], AND JESSY W. GRIZZLE[2], (Fellow, IEEE)

[1]Department of Mechanical Engineering, Carnegie Mellon University, Pittsburgh, PA 15213, USA
[2]Department of Electrical Engineering and Computer Science, University of Michigan, Ann Arbor, MI 48109, USA
[3]Department of Mechanical and Civil Engineering, California Institute of Technology, Pasadena, CA 91125, USA
[4]Wandercraft SAS, 75017 Paris, France
[5]MINES ParisTech, PSL Research University, 77300 Fontainebleau, France
[6]Centre Automatique et Systèmes, École des Mines de Paris, PSL Research University, 77300 Fontainebleau, France

Corresponding Authors: Ayush Agrawal (ayusha@andrew.cmu.edu) and Omar Harib (omar.harib@outlook.com)

The first two authors contributed equally. The work of A. Agrawal and K. Sreenath was supported by NSF under Grant IIS-1526515. The work of O. Harib and J. W. Grizzle was supported by NSF under Grant NRI-1525006. The work of A. Hereid was supported by NSF under Grant CPS-1239037. The work of A. D. Ames was supported by NSF under Grant IIS-1526519.

ABSTRACT This paper presents preliminary results toward translating gait and control design for bipedal robots to decentralized control of an exoskeleton aimed at restoring mobility to patients with lower limb paralysis, without the need for crutches. A mathematical hybrid dynamical model of the human-exoskeleton system is developed and a library of dynamically feasible periodic walking gaits for different walking speeds is found through nonlinear constrained optimization using the full-order dynamical system. These walking gaits are stabilized using a centralized (i.e., full-state information) hybrid zero dynamics-based controller, which is then decentralized (i.e., control actions use partial state information) so as to be implementable on the exoskeleton subsystem. A control architecture is then developed so as to allow the user to actively control the exoskeleton speed through his/her upper body posture. Numerical simulations are carried out to compare the two controllers. It is found that the proposed decentralized controller not only preserves the periodic walking gaits but also inherits the robustness to perturbations present in the centralized controller. Moreover, the proposed velocity regulation scheme is able to reach a steady state and track desired walking speeds under both, centralized, and decentralized schemes.

INDEX TERMS Exoskeletons, control design, robot control.

I. INTRODUCTION

Exoskeletons for lower limbs are wearable robotic devices that fit around the legs and pelvis of a user. These may serve as either *Human Performance-Augmenting* devices [15], [26], [33], [42], [46]– designed to help improve strength and endurance of able-bodied persons, typically for military and industrial applications or as orthotic devices [9], [14], [29], [37] – to assist physically challenged persons. A comprehensive review of the state-of-the-art lower limb exoskeletons can be found in [13]. The focus of this work is to design controllers for full lower limb exoskeletons to restore normal ambulatory functions in patients with lower limb paralysis and allow free motion without the use of crutches. These include patients with spinal cord injuries who have lost muscle function in the lower half of their body.

Research on full lower limb active exoskeletons for orthosis dates back to as early as the 1960's when exoskeletons designed to restore mobility in paraplegics were being developed separately at the Mihailo Pupin Institute in Belgrade [24], [38] and at the University of Wisconsin [21], [34]. Regularly since then, medical interest in exoskeletons has increased with the understanding of their potential to provide autonomy to handicapped people and commercial products have been used within rehabilitation centers for paraplegic patients since at least 2011, with new products and new treatments regularly approved by the US Food and Drug Administration.

The first exoskeletons, nevertheless, have limitations: either they do not provide autonomous walking, requiring crutches for stability and direction [1], [3], or only allow

FIGURE 1. Image of Exoskeleton from Wandercraft. Link names with respective mass values are presented in Table 1.

quasi-static gaits with velocities on the order of 3 m/min [4]. Overcoming these limitations means having exoskeletons able to perform dynamic walking in controlled settings—known environment, known user—without external assistance, thereby providing greater autonomy to users. This is for example what the startup Wandercraft is currently developing [5], namely a 12 degree of actuation exoskeleton, see 1. It is intended to allow for dynamic walking, at first in medical center settings.

More recently, in an effort to provide a platform for the development of such biomechatronic devices, ETH Zurich conducted a one-of-a-kind race for people with disabilities using powered assistive devices, which included wheelchairs, arm and leg prosthesis and robotic exoskeletons [2]. The powered exoskeleton race saw participation from eight teams and participants were asked to complete as many tasks as possible in a given time frame, which included sitting down on and standing up from a chair, walking around static obstacles (slalom course), walking over ramps and navigating through doorways, walking across tilted tiles and over discrete footholds (stepping stones).

The next generation of exoskeletons will be designed to adapt to unknown environments and operate with minimal initial information regarding the user. Mobility will then move beyond walking, to include features such as standing, sitting, climbing stairs, avoiding obstacles or getting back-up from a fall. Open-loop control algorithms will not suffice for this new generation of exoskeletons, which motivates the search for new control algorithms. To reach the expected level of performance, it seems natural to take inspiration from control techniques developed for bipedal robots.

In the area of bipedal robots, tools are being developed that allow very rapid design of model-based feedback controllers, that respect torque limits, friction cone constraints, joint speeds, and gait characteristics, such as foot height clearance and walking speed, while allowing for uncertainty in the model and the environment [16], [19], [23], [31], [41]. The objective of this paper is to begin the process of translating these recent advances from bipedal walking robots to exoskeletons [35].

Similar to cited work on bipeds, the full-order dynamical model is used both in the control design and in trajectory optimization. The model includes the full dynamics of the exoskeleton in addition to a simplified model of the human upper body. The actuators used in the exoskeleton are high-fidelity electric motors. While there is a body of work on high-accuracy control of motors [43], it has been observed from recent work in bipedal robots with similar actuation that simply modeling such motors as torque sources, with the reflected inertia being part of the dynamical model, provides an adequate dynamical representation of the system, as seen from work in [10], [11], [19], [23], and [32].

Control schemes from bipedal robotic locomotion are typically *centralized*, meaning that there is a single controller with complete knowledge of the system. In the case of an exoskeleton and user, such complete knowledge would require the full state of the user and the exoskeleton, as well a complete dynamical model of the human and robot, an obviously impractical assumption. This requires us to think about a *decentralized* control architecture, that is, a control architecture [22] that requires a realistic amount of information about, and shared between, the human and exoskeleton subsystems so that robust walking can still be realized. Importantly, results on translating centralized robotic walking to decentralized prosthetic locomotion have recently proved successful [18], [44], [45], pointing toward the possibility of similar results in the context of exoskeletons.

Control of biomechatronic devices that augment humans, such as prostheses and exoskeletons, for bipedal locomotion share many of the challenges of bipedal robot locomotion, such as, nonlinear and hybrid dynamics, high degree of underactuation, and input constraints on actuators. Additional challenges that are specific to these biomechatronic devices include the ability to handle interaction forces between the human and the robotic device, and being robust to uncertainty in the human dynamical parameters, such as variation in mass and inertia parameters among different subjects, or the user moving his or her arms in an unplanned manner.

The particular control method studied here is based on virtual holonomic constraints and hybrid zero dynamics. Virtual holonomic constraints, or virtual constraints for short, are relations between the joints or links of a device that are induced by feedback control instead of a physical connection. The hybrid zero dynamics (HZD) are a reduced order dynamical model of the system that is induced by the virtual constraints. This control design method is selected because of the large body of analytical and experimental work that has been developed around it [16], [19], [23], [31], [41].

In this paper, we develop a nonlinear decentralized controller for a lower extremity exoskeleton. The primary contributions of this paper with respect to prior work are:

- Generation of natural walking gaits that are dynamically feasible for the human-exoskeleton system that enforce the unilateral ground contact as well as friction and input torque constraints.
- Design of a control architecture allowing the human to actively control and regulate the walking velocity of the human-exoskeleton system using his torso.

- Design of a decentralized controller, with minimal sharing of sensing information between the human and exoskeleton subsystems, that not only preserves the periodic orbit created by a centralized HZD controller, but is also robust to perturbations.
- Numerical validation of the proposed controller on a 21 degrees-of-freedom (DOF) human-exoskeleton system walking at speeds ranging between 0.13 m/s and 0.34 m/s, and being sufficiently robust to walk on ramps of up to 5° slopes.

The remainder of the paper is organized as follows. Section II presents a hybrid, nonlinear model of the human-exoskeleton system. In Section III a centralized HZD-based controller is presented. In Section IV a velocity regulation scheme, that allows the human subject to control velocity of the exoskeleton, is presented. Section V presents a decentralized version of the HZD controller for the human-exoskeleton subsystems. Section VI presents results of numerical simulations and compares the two controllers. Finally, Section VII provides concluding remarks.

II. HYBRID MODEL OF WALKING

Having presented the state-of-the-art in lower limb exoskeletons and introduced the challenges in control design of these devices, in this section, we develop a hybrid dynamical model of the human exoskeleton system. Particularly, we model the various links of the exoskeleton and the torso and arms of the human as rigid links connected by revolute joints.

Remark 1: In our model, we assume that the human lower body and the exoskeleton can be treated as a lumped system, with no actuation from the human legs. This is a reasonable assumption to make since the purpose of this paper is to develop exoskeleton controllers for patients with complete lower limb paralysis. Patients with paralysis, however, may develop spasticity resulting in sudden and involuntary actions. The effect of forces from the human lower limbs will be considered in a future publication.

Depending upon the nature of interaction with the environment, bipedal locomotion, such as walking and running, can be decomposed into several individual phases (or domains). Each domain can be described by a continuous phase followed by a discrete event, triggering the transition to the next domain. In the following paragraphs, we develop a hybrid model of *3D flat-footed* walking with actuated feet, characterized by a continuous swing phase and an instantaneous double support phase.

A. HYBRID DYNAMICAL MODEL

To construct the hybrid model of the system, we employ techniques detailed under [20, Sec. 4]. Specifically, we use floating base coordinates to represent the configuration variables, $\mathcal{Q}$, of the system, i.e. $q = (p, \phi, q_b) \in \mathcal{Q} = \mathbb{R}^3 \times SO(3) \times \mathcal{Q}_b$ represents the generalized coordinates of the system, where $p \in \mathbb{R}^3$ and $\phi \in SO(3)$ represent the Cartesian position and orientation of the body-fixed frame with respect to the inertial frame respectively and $q_b \in \mathcal{Q}_b \subset \mathbb{R}^n$ represents the set of body coordinates (joint angles).

TABLE 1. Exoskeleton links with Masses.

	Link Name	Link Mass (kg)
Human subsystem	Pelvis	7.84
	Waist	26.94
	Torso	13.35
	Arm	3.5
Human-Exoskeleton system	Hip Link (frontal plane)	3.45
	Hip Link (transverse plane)	0.75
	Hip Link (sagittal plane)	14.68
	Knee Link	8.92
	Ankle Link (sagittal plane)	1.33
	Ankle Link (frontal plane)	0.96
	Toe Link	0.63
	Total Mass	**116.5**

The Lagrangian of the system, $\mathcal{L} : T\mathcal{Q} \to \mathbb{R}$ is given as the difference between the total kinetic energy, $T : T\mathcal{Q} \to \mathbb{R}$, and the potential energy, $V : \mathcal{Q} \to \mathbb{R}$, i.e. $\mathcal{L}(q, \dot{q}) = T(q, \dot{q}) - V(q)$, where $T\mathcal{Q}$ represents the tangent space of $\mathcal{Q}$.

1) HOLONOMIC CONSTRAINTS

Any physical contact with the external environment is modeled as a holonomic constraint, $\eta_c : \mathcal{Q} \to \mathbb{R}$, a function of the configuration variables alone. For each domain, the holonomic constraints are held constant, i.e. $\eta_c \equiv$ constant, and the associated kinematic constraint is $J(q)\dot{q} = 0$. Here $J(q)$ is the Jacobian of the holonomic constraint, i.e. $J(q) = \partial \eta_c / \partial q$.

2) CONTINUOUS DYNAMICS

The continuous dynamics is obtained by solving the Euler-Lagrange equations and can be expressed in the form of the standard *manipulator equations*:

$$D(q)\ddot{q} + H(q, \dot{q}) = Bu + J^T(q)F, \tag{1}$$

where $D(q)$ is the inertia matrix, $H(q, \dot{q}) = C(q, \dot{q})\dot{q} + G(q)$ is the vector containing the sum of the Coriolis and gravity term, B is the actuator distribution matrix, and $F : T\mathcal{Q} \times U \to \mathbb{R}^{n_c}$ is a vector of contact *wrenches* containing the contact constraint forces and/or moments (see [28]), where n_c is the number of holonomic constraints, and $u \in U$, is the control input. The contact wrenches, F, can be obtained by solving the second derivative of the holonomic constraints,

$$J(q)\ddot{q} + \dot{J}(q, \dot{q})\dot{q} = 0, \tag{2}$$

and (1) simultaneously. Substituting the closed form solution of F into (1) yields the control affine, nonlinear continuous dynamics, $\dot{x} = f(x) + g(x)u$, where $x = (q, \dot{q}) \in \mathcal{TQ}$, represents the state of the system.

3) DOMAIN OF ADMISSIBILITY

In order for the holonomic constraints to be satisfied, a set of constraints must be enforced on the contact forces [20], [25]. These conditions are stated in the form of inequalities as

$$\nu(q)F(q, \dot{q}, u) \geq 0, \tag{3}$$

where $\nu(q)$ depends on the physical parameters of the system (e.g. geometry of foot, friction coefficient with the ground). An example of such a constraint is that the ground reaction forces must lie within the friction cone.

A different type of constraint that determines the admissible configurations of the system are known as *unilateral constraints* and denoted by $h(q) > 0$. For example, constraints like the non-stance foot must always be above the ground during swing phase, fall under this category. The domain of admissibility is then defined as the set of states and control inputs where the holonomic and unilateral constraints are satisfied [20], namely

$$\mathcal{D} = \{(q, \dot{q}, u) \in T\mathcal{Q} \times U \mid A(q, \dot{q}, u) \geq 0\}, \tag{4}$$

where

$$A(q, \dot{q}, u) = \begin{bmatrix} \nu(q)F(q, \dot{q}, u) \\ h(q) \end{bmatrix} \geq 0. \tag{5}$$

4) GUARDS

A switching surface or guard, is a proper subset of the boundary of the domain of admissibility. Let $H(q, \dot{q}, u)$ be the appropriate elements from the vector in (5) corresponding to the edge condition. Then the guard is defined as

$$S = \{(q, \dot{q}, u) \in T\mathcal{Q} \times U | H(q, \dot{q}, u) = 0, \dot{H}(q, \dot{q}, u) < 0\}. \tag{6}$$

5) DISCRETE DYNAMICS

Associated with the guard, S, is an impact map, $\Delta : S \to Q$, a smooth function that maps pre-impact states, $(q^-, \dot{q}^-)$, to states post impact, $(q^+, \dot{q}^+)$. Moreover, post-impact configurations remain the same since the configuration of the system is invariant to impacts. The post-impact configuration velocities, however, need to satisfy the plastic impact [20],

$$\begin{bmatrix} D(q) & -J^T(q) \\ J(q) & 0 \end{bmatrix} \begin{bmatrix} \dot{q}^+ \\ \delta F \end{bmatrix} = \begin{bmatrix} D(q)\dot{q}^- \\ 0 \end{bmatrix}. \tag{7}$$

The hybrid model of the overall system depicted in Fig. 2 is comprised of the continuous-time dynamics and the discrete reset map,

$$\Sigma : \begin{cases} \dot{x} = f(x) + g(x)u, & x \notin S, \\ x^+ = \Delta(x^-), & x \in S. \end{cases} \tag{8}$$

The floating base model of the overall system has 21 DOF, with six of those corresponding to the floating base. The system has 15 degrees of actuation, with 12 actuators for the exoskeleton and three for the human.

III. CENTRALIZED CONTROLLER FOR BIPEDAL WALKING

Having developed the hybrid dynamical model of the human-exoskeleton system, we next present a feedback controller to achieve dynamic walking. In particular, this will be a centralized controller that has been successfully implemented on high DOF underactuated 3D bipedal robots [23], [32], [36]. An identifying feature of the control method is that the various links of the robot are coordinated by a single phase variable that depends on the robot state only and is independent of time. This method has been successfully translated to lower limb prosthesis [18], [45].

A. VIRTUAL CONSTRAINTS

At the core of our controller approach is designing a set of outputs, $y(x)$, known as virtual constraints, such that the zeroing of these outputs leads to the desired robot behavior. In other words, virtual constraints are functions of the state variables that define how the various links of the robot should move. These virtual constraints are regulated via feedback control rather than through mechanical linkages, and hence the name virtualİ constraints.

These virtual constraints are formulated as the difference between their actual values, y^a, and desired values, y^d, yielding

$$y = y^a - y^d. \tag{9}$$

For the particular case of 3D flat-footed walking, we chose the outputs, y^a, to be a combination of velocity regulating terms, y_1^a and position modulating terms, y_2^a, i.e. $y^a = [y_1^a; y_2^a]$ where y_i^a is a relative degree i output, $i \in \{1, 2\}$.

We choose $y_1^d = v_d \in \mathbb{R}$ to be the corresponding desired velocity and choose

$$y_2^d = y_2^d(\tau(q, \beta), \alpha) \tag{10}$$

as the desired relative degree two output described by a set of parameters, α, and *phase variable*, τ, a monotonically increasing function of the configuration variables, q, and parameters, $\beta = (\beta_1, \beta_2)$. Here, the phase variable is defined as

$$\tau(q, \beta) := \frac{\delta p_{hip}(q) - \beta_2}{\beta_1 - \beta_2} \in [0, 1], \tag{11}$$

where δp_{hip} is the horizontal hip position relative to the stance foot position in the sagittal plane (see Fig. 2). Note that τ is normalized to be within [0, 1]. The scaling vector (β_1, β_2) is defined as

$$(\beta_1, \beta_2) := (\delta p_{hip}(q_0), \delta p_{hip}(q_f)), \tag{12}$$

where q_0 and q_f define the configuration of the human-exoskeleton system at the beginning and end of a step.

For the relative degree two virtual constraints, we use Bézier polynomials to parametrize the desired evolution as a function of the phase variable, τ,

$$y_2^d(\tau, \alpha) := \sum_{k=0}^{M} \alpha[k] \frac{M!}{k!(M-k)!} \tau^k (1-\tau)^{M-k}, \tag{13}$$

where M is the order of the Bézier defined by $M + 1$ coefficients. The tuple $\{\alpha, \beta, v_d, x^{\mathcal{O}}\}$ then defines a gait.

Remark 2: For the human-exoskeleton system, the following virtual constraints are defined in terms of actuated joints and are hence in body coordinates: Stance Knee Pitch, Stance Hip Roll, Stance Ankle Roll, Stance Hip Yaw, Stance Pelvis

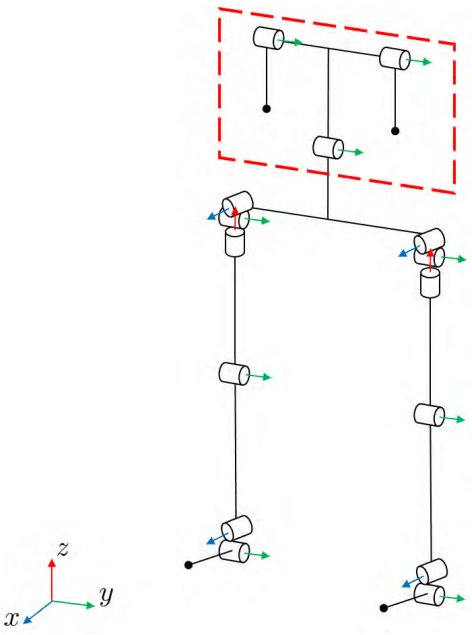

FIGURE 2. Kinematic tree for the modeled human-exoskeleton system. The *xz*-plane will be called hereafter the sagittal plane, *yz* the frontal plane and and *xy* the transverse plane. The red dotted box outlines the human subsystem.

Pitch, Stance Arm Pitch, Torso Pitch, Swing Arm Pitch, Swing Knee Pitch, Swing Hip Roll and Swing Hip Pitch. The following virtual constraints, on the other hand, are defined in terms of world-frame orientation: Swing Foot Roll, Swing Foot Pitch and Swing Foot Yaw. For the each of these 14 virtual constraints, the actuator torques show up in their second derivatives and hence are said to be relative degree two and are denoted as y_2*. The remaining virtual constraint is defined as the horizontal velocity of the hip; the torques show up in the first derivative of this virtual constraint; it is therefore said to be relative degree one and is denoted by* y_1*. Note that we have defined 15 virtual constraints corresponding to the 15 actuators in the human-exoskeleton system.*

B. PARTIAL HYBRID ZERO DYNAMICS AND A CENTRAL CONTROLLER

Having established a hybrid dynamical model of walking and presented a set of virtual constraints that needs to be enforced, we use feedback techniques developed in [41] to enforce these constraints. This creates a partial hybrid zero dynamics surface (partial HZD) [7] embedded in the state space. The developed controller is a centralized controller in the sense that it requires full knowledge of the entire state vector. More details on partial hybrid zero dynamics and the centralized controller have been relegated to Appendix I.

C. GAIT GENERATION VIA DIRECT COLLOCATION METHOD

For the HZD method of control design, we need to design the desired profile of the virtual constraints that when enforced leads to a stable walking gait. This is done through a nonlinear constrained optimization process using direct collocation [23]. Further details on the direct collocation based optimization are presented in Appendix II, while the constraints that are enforced by the optimization are presented in Appendix III.

The result from the optimization is the set of parameters $\{\alpha, \beta, v_d, x^{\mathcal{O}}\}$ which fully describes an individual gait, where $x^{\mathcal{O}}$ is the evolution of the states of the system along the orbit $\mathcal{O}$ parametrized by τ, while α, β, v_d are as defined previously. The stability of the resulting gait can be inferred as in [41, Th. 5.3], or as we will do later, by directly computing the Poincaré map.

IV. VELOCITY REGULATION

Having presented the continuous-time HZD controller and the nonlinear constrained optimization to generate periodic gaits, we now present a method to enable walking velocity regulation based on the desired human velocity. In particular, this section presents a convenient means for the user to vary the walking speed of the exoskeleton, while maintaining stability and satisfying torque, ZMP[1] and friction constraints. The key ideas are: (1) to design a discrete library of gaits and controllers for stable walking at fixed speeds; (2) to interpolate the gaits and controllers to create a continuum of walking gaits and controllers [11]; and (3) for the user to command speed increases or decreases through his or her torso lean angle, similar to how one rides a Segway. Each of these aspects of the speed regulation is addressed in the following.

A. LIBRARY OF GAITS

To regulate the velocity of the exoskeleton, a method similar to [11] is used. A finite library of gaits, $\mathfrak{L}$, is generated through optimization for different desired walking speeds v_d. The step duration is restricted to around 0.8 (s) and all physical constraints discussed in Sect. VII are imposed. Each gait in the library $\mathfrak{L}$ is defined by the parameters $\{\alpha, \beta, v_d, x^{\mathcal{O}}\}^i := \{\alpha, \beta, v_d, x^{\mathcal{O}}\}(v_d^i)$, all of which were defined in III-A. The gaits are ordered by increasing values of v_d^i. Gaits were generated for values of

$$\{v_d^1, \cdots, v_d^7\} = \{0.13, 0.15, 0.18, 0.20, 0.24, 0.29, 0.34\} \text{ m/s}. \quad (14)$$

Gait parameters at an intermediate speed v are generated by linearly interpolating the gait library. Specifically,

$$\zeta = \frac{v - v_d^i}{v_d^{i+1} - v_d^i}, \; v_d^i \leq v < v_d^{i+1}, \quad (15)$$

[1]The Zero Moment Point (ZMP) is a point in the contact region of the stance foot and the ground where the sum of all moments of active forces with respect to this point is equal to zero. The ZMP constraint enforces that the ZMP is within, and not at the boundary of, the foot geometry.

$$\left\{\alpha, \beta, v_d, x^{\mathcal{O}}\right\}(v) = (1-\zeta) * \left\{\alpha, \beta, v_d, x^{\mathcal{O}}\right\}^{i} + \zeta * \left\{\alpha, \beta, v_d, x^{\mathcal{O}}\right\}^{i+1}, \quad (16)$$

where $\zeta \in [0, 1]$ is the interpolation factor and the parameters for the interpolated gait are $\left\{\alpha, \beta, v_d, x^{\mathcal{O}}\right\}(v)$ with $v_d = v$.

Remark 3: To be extra clear, in the above equations the parameters $\{\alpha, \beta, v_d, x^{\mathcal{O}}\}$ vary continuously with the velocity v.

TABLE 2. Dominant eigenvalues at different speeds.

Forward Velocity (m/s)	Largest Eigenvalue
0.17	0.3023
0.19	0.2150
0.21	0.3606
0.23	0.3313
0.25	0.1891
0.27	0.1764

This then creates a continuum of gaits, each of which is locally exponentially stable and meets the design constraints given in Sect. VII, see [11] for reasons on why this is true. To demonstrate this, we numerically compute the Poincare map as described in [41] and tabulate the modulus of the dominant eigenvalue of the linearized Poincare map in Table 2 for different interpolated speeds. Since these values are strictly less than 1, the gaits are locally exponentially stable, see [41] for more details.

B. RELAXING LOCAL STABILITY OF WALKING SPEED

The above gaits, being asymptotically stable, will reject attempts by the user to change the walking speed through body posture adjustments. We now prepare the controller to more readily accept such posture changes as speed commands from the user.

Let $y_1^a(x^-)$ be the longitudinal velocity of the exoskeleton's hip at the end of the current step. When selecting a gait for the next step, suppose that we set v in (15) and (16) such that $v = y_1^a(x^-)$. Then, as explained in [11], two things will happen. First of all, we are selecting a gait that respects important physical constraints around the system's current walking speed. Secondly, the closed-loop system becomes "neutrally stable" in the sense that all but one of the eigenvalues of the Jacobian of the Poincaré map are strictly within the unit circle, and the remaining eigenvalue is approximately equal to one. In other words, when looking at the system step to step, the longitudinal speed behaves like an integrator because the controller's setpoint at each step is reset to the speed of previous step. Said another way, if a "disturbance" or "user command" causes the system to increase or decrease walking speed over the course of a step, the new speed will be maintained during the next step. The next subsection will show this to be a highly desirable property for the closed-loop system as it makes it easy for the user to regulate speed through torso pitch angle.

C. USER REGULATION OF WALKING SPEED

With the exoskeleton being controlled to walk at a continuum of velocities, but being neutrally stable in the sense described above, a means is now provided for the user to stabilize the walking speed to a desired value. This is accomplished by having the human command speed changes to the exoskeleton through changes in torso pitch angle.

The basic idea can be inferred from how a human regulates the speed of a Segway: a forward lean of the body accelerates the Segway, while a backward lean decelerates it. Here, a change in the user's torso pitch with respect to the upright position will be interpreted as a desired increment (or decrement) of the walking speed with respect to the current walking speed. Speed increase or decrease over the course of a step is a discrete-time or hybrid analogue to acceleration or deceleration of a Segway. Both allow velocity regulation to be accomplished with a proportional control actions that humans master easily.

The speed regulation policy described above is implemented through a simple modification of the outer-loop of the exoskeleton controller. Specifically, at the end of each step, the desired velocity is modified to take into account the user's torso angle,

$$v = y_1^a(x^-) + \delta v \quad (17)$$

$$\delta v := K_v * (q_T^a - 0), \quad (18)$$

where v is the velocity used to select a gait as seen in (15) and (16), K_v is a proportional gain, and q_T^a is the user's torso pitch angle at the end of the previous step.

D. SIMPLE MODEL OF USER CONTROL ACTIONS

For the purpose of simulating a user walking in the exoskeleton, we need to model how the user will modify their torso pitch angle step-to-step when signaling desired speed changes to the exoskeleton. The simple proportional controller

$$q_T^d := K_t * (v_{H,d} - y_1^a(x^-)) \quad (19)$$

is assumed, where q_T^d is the desired torso angle to be achieved at the end of the next step, K_v is a proportional gain, $v_{H,d}$ is the velocity desired by the human.

The proportional controller could be replaced with a more advanced policy, such as one having integral and derivative terms to better reflect a more highly trained user, though this is not done here. We choose instead to focus on smooth transitions in the desired speeds. The following assumptions are made on how the human moves the torso. These properties could be achieved through training, or modifications could be added to the exoskeleton controller to achieve the same objectives:

- The path of the torso can be captured by Bézier polynomial that starts at the current torso angle and ends at the desired angle, with a starting and ending slope of zero.
- To avoid large jumps in velocity, q_T^d and δv are saturated. The gains and saturations used in this exoskeleton are as

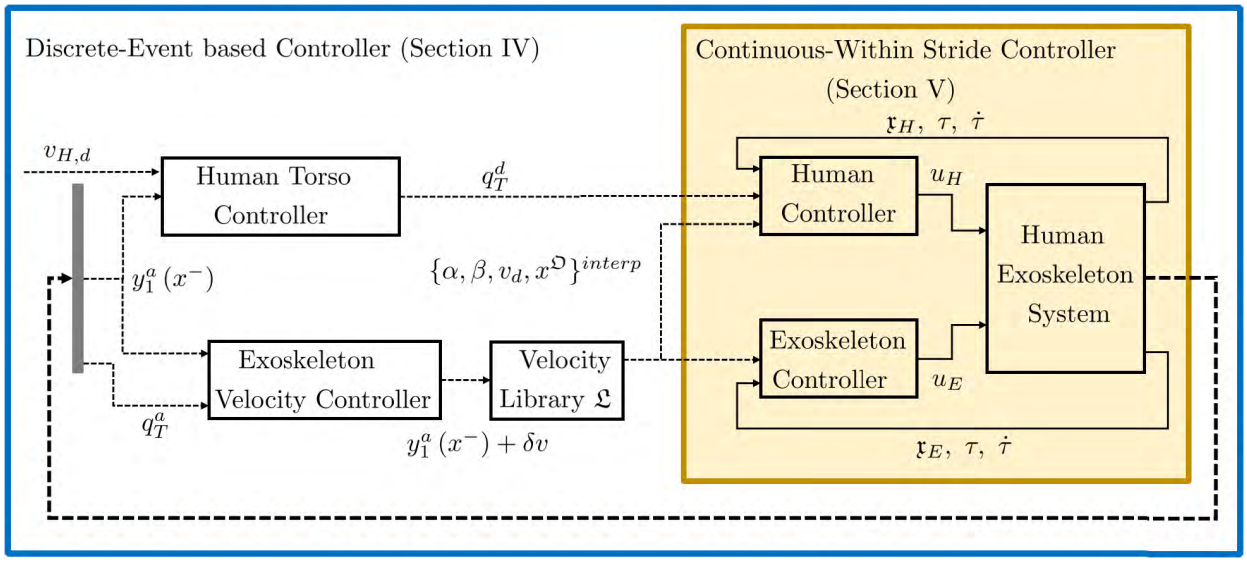

FIGURE 3. Feedback diagram illustrating the decentralized controller with velocity regulation. Block in yellow denotes continuous-time, decentralized controller. Block in blue denotes the discrete-time event-based velocity regulation controller, executed at the end of every walking step. Dashed lines denote variables sampled at the end of every step.

follows:

$$\begin{aligned} -0.06 \text{ m/s} \leq \delta v &\leq 0.06 \text{ m/s} \\ -5^\circ \leq q_T^d &\leq 5^\circ \\ K_t &= 0.5 \text{ rads/m} \\ K_v &= 0.7 \text{ m/(s rad)}. \end{aligned}$$

Remark 4: It was found that $K_t K_v \leq 0.5$ results in good velocity regulation with periodic motion in steady state. Lower values result in slower tracking of the desired velocity. Note that the expression $K_t K_v$ arises when we substitute (19) *into* (18) *with $q_T^a \approx q_T^d$.*

V. DECENTRALIZED CONTROLLER

Having presented HZD-based control design for bipedal walking and a means for the human user to control the velocity of the exoskeleton, we now introduce a decentralized control architecture for the human-exoskeleton system. The need for decentralization is motivated by the fact that it is often difficult or impractical to obtain precise state information of the human, which involves attaching sensors to various links and joints of the human pilot. Also, it is possible that the human pilot may not know what the true state of the exoskeleton system is. This motivates us to develop a decentralized controller that minimizes the sensing information that is shared between the human subject and the exoskeleton. Towards this, we first present assumptions we make about the information available to the human and the exoskeleton controllers, followed by the decentralized controller. An overview of the decentralized control design with the velocity regulation approach is presented in Fig. 3. Note that the two control inputs (u_H, u_E) from the decentralized controller are only needed for simulations in which the human behavior is being represented through simulation. In practice only u_E is implemented on the exoskeleton system with the real human taking over for u_H.

A. CONTROL DESIGN ASSUMPTIONS

1) *State Decomposition*: The state of the human-exoskeleton system, x, can be decomposed into states of the human, exoskeleton and global variables,

$$x = [x_H; x_E; x_G],$$

where, $x_H \in \mathbb{R}^h$ represents the states corresponding to the human configuration variables and are available to the human alone. In the human model, these correspond to the human torso and arm joints. Similarly, $x_E \in \mathbb{R}^e$ represents the states corresponding to the configuration variables of the exoskeleton and are available to the exoskeleton controller alone. The global state variables, $x_G \in \mathbb{R}^g$ are available to both, the human as well as the exoskeleton controller. These pertain to the position and orientation of the system with respect to an inertial frame of reference. Here h, e and g are positive constants such that, $h + e + g = n$.

2) *Existence of Periodic Orbit*: There exists an asymptotically stable periodic orbit, $\mathcal{O}$, for the closed-loop system, Σ in (8), with the input-output linearizing controller, u_{IO}.

3) *Partial State Information*: With the exception of the assumptions 5a and 5b, it is assumed that the human subsystem has knowledge only about the human and global states, x_H, x_G, and assumes the corresponding exoskeleton states are always on the periodic orbit, $\mathcal{O}$. Similarly, the exoskeleton subsystem has information only about the exoskeleton and global states, x_E, x_G, and assumes that the states corresponding to the human are

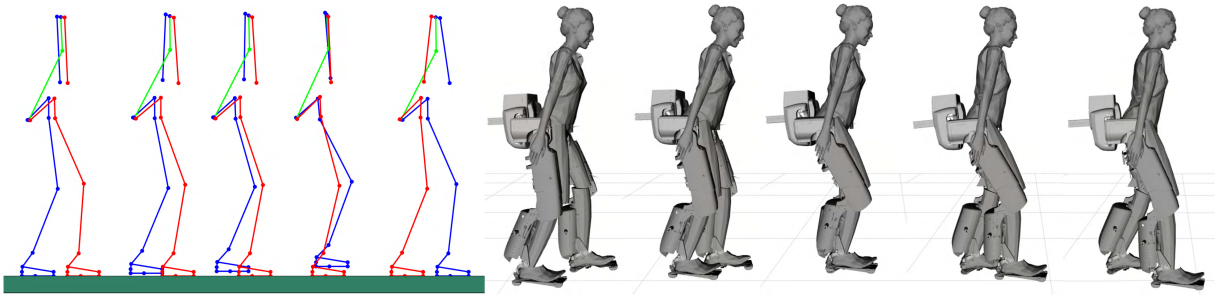

FIGURE 4. Snapshots of walking at a desired speed of 0.3 m/s achieved by our proposed controller on the human-exoskeleton system is shown. An animation video of the simulation is available at https://youtu.be/VXP7DKY6Trc.

always on the periodic orbit, $\mathcal{O}$. Therefore, the variables available to the human controller, $\mathfrak{x}_H$, and the exoskeleton controller, $\mathfrak{x}_E$ are given by,

$$\mathfrak{x}_H = [x_H; x_E^{\mathcal{O}}; x_G],$$
$$\mathfrak{x}_E = [x_H^{\mathcal{O}}; x_E; x_G],$$

where, $x_E^{\mathcal{O}} \in \mathbb{R}^e$ and $x_H^{\mathcal{O}} \in \mathbb{R}^h$ represent the states corresponding to the exoskeleton and human joints on the periodic orbit, respectively.

It should be noted that $x_H^{\mathcal{O}}$ is simply the human having an upright stance relative to the exoskeleton with downright arms, since the exoskeleton is unaware of the motion of the human torso in the middle of a step.

Remark 5: The human would be controlling their torso angle to adjust their speed. In addition, the human is expected to use their arms and not hold it statically. This implies that the true human state $x_H \neq x_H^{\mathcal{O}}$. Still, it is believed that a sufficiently robust controller on the exoskeleton would keep the system stable, despite not having the light human upper body on their periodic orbit. In addition, with the exoskeleton accelerating or decelerating, the exoskeleton won't always be on its periodic orbit either. With that, it is assumed that the human would be able to track their desired torso pitch angles regardless of the state of the exoskeleton. Section VI will show how the system behaves under small steady state errors in the torso tracking.

4) *Phase Variable*: The phase variable, τ is available to the exoskeleton controller. If one models the human's controller for posture and arm regulation as being synchronized with the gait, then one may assume that τ is also available to the human. Here, we use τ to generate a feedforward term for regulating the posture of the upper body (torso and arms).
5) *Velocity Regulation*:
   a) In between steps, for purposes of computing q_T^d, the human has access to $y_1^a(x^-)$, the linearized hip velocity at the end of the previous step before impact.
   b) In between steps, for purposes of computing δv, the exoskeleton has access to q_T^a, the relative torso angle at the end of the previous step.
6) *System Model*: The human and the exoskeleton controller have knowledge about the actual model of the system.

B. DECENTRALIZED CONTROL DESIGN

Note that, throughout this section, the indexing variable, $i \in \{H, E\}$ corresponds to the human or exoskeleton and the indexing variable, $k \in \{1, 2\}$ denotes relative degree one or relative degree two.

We begin by obtaining the desired outputs, v_d and $y_2^d(\tau, \alpha)$, representing a walking gait through constrained nonlinear optimization using direct collocation methods, detailed in Section III-C, for the complete human-exoskeleton system.

The control equations we develop next closely follow that introduced in Section III, with states $\mathfrak{x}_i$ and outputs y_i. In particular, we compute the vector fields, $f(\mathfrak{x}_i)$ and $g(\mathfrak{x}_i)$, outputs, $y_i = [y_{1,i}; y_{2,i}]$, and the Lie derivatives, $L_f^k y_{k,i}$ and $L_g L_f^{k-1} y_{k,i}$ corresponding to the human states, $\mathfrak{x}_H$, and exoskeleton states, $\mathfrak{x}_E$ where,

$$y_i = \begin{bmatrix} y_{1,i} \\ y_{2,i} \end{bmatrix} := \begin{bmatrix} y_1^a(\mathfrak{x}_i) - v_d \\ y_2^a(\mathfrak{x}_i) - y_2^d(\tau, \alpha) \end{bmatrix}.$$

Note that, to better use the available measurements of $\tau, \dot{\tau}$ as per Assumption 4 in Sec. V-A, the decentralized controller computes the Lie derivatives as follows:

$$\begin{aligned} L_f y_{k,i}(\tau, \dot{\tau}, \mathfrak{x}_i) &= L_f y_k^a(\mathfrak{x}_i) - \frac{\partial y_k^d}{\partial \tau}(\tau, \alpha)\dot{\tau}, \\ &= L_f y_k^a(\mathfrak{x}_i) - \dot{y}_k^d(\tau, \dot{\tau}, \alpha), \\ L_f^2 y_{2,i}(\tau, \dot{\tau}, \mathfrak{x}_i) &= L_f^2 y_2^a(\mathfrak{x}_i) - \frac{\partial \dot{y}_2^d(\tau, \dot{\tau}, \alpha)}{\partial \tau}\dot{\tau} \\ &\quad - \frac{\partial \dot{y}_2^d(\tau, \dot{\tau}, \alpha)}{\partial \dot{\tau}} L_f \dot{\tau}(\mathfrak{x}_i), \\ L_g L_f y_{2,i}(\tau, \dot{\tau}, \mathfrak{x}_i) &= L_g L_f y_2^a(\mathfrak{x}_i) \\ &\quad - \frac{\partial \dot{y}_2^d(\tau, \dot{\tau}, \alpha)}{\partial \dot{\tau}} L_g \dot{\tau}(\mathfrak{x}_i). \end{aligned}$$

Two separate control inputs, for the human (u_H) and for the exoskeleton (u_E), are computed as follows,

$$u_{IO,i} = \mathcal{A}_i^{-1} \left(\begin{bmatrix} L_f y_{1,i}(\mathfrak{x}_i) \\ L_f^2 y_{2,i}(\mathfrak{x}_i) \end{bmatrix} + \begin{bmatrix} \mu_{1,i} \\ \mu_{2,i} \end{bmatrix} \right)$$
$$u_i = T_i \cdot u_{IO,i}.$$

TABLE 3. List of variables pertaining to the controller design, velocity regulation, and decentralized controller.

Variable	Description
y, y_1, y_2, y^a, y^d	y are the set of virtual constraints imposed by the controller, where $y = y^a - y^d$. y^a is the actual values of a set of outputs from the system while y^d is the desired values for the outputs. y_1 and y_2 define relative degree one and two virtual constraints respectively.
α, β, τ	α is a set of Bèzièr polynomial coefficients used to define y_2^d. The polynomials are parametrized by the phase variable $\tau \in [0, 1]$ where τ is a function of the state of the system. β is a set of parameters used to compute τ. During a step τ should be monotonically increasing.
$x^{\mathcal{O}}$	The evolution of the states of the system along a periodic orbit $\mathcal{O}$ as a function of τ.
$\mathfrak{L}$	Ordered set of gait primitives in increasing order of desired hip velocity y_1^d
$\{\alpha, \beta, v_d, x^{\mathcal{O}}\}^{next}$	Set of gait parameters for the next step.
$y_1^a(x^-)$	The actual linearized hip velocity at the end of the previous step
$v_{H,d}$	The desired speed the human wants to achieve
q_T^d	The desired torso angle, chosen by the human, to be achieved by the end of the next step
q_T^a	The actual relative torso pitch angle at the end of the previous step
δv	Change in the desired hip velocity of a gait (away the periodic gait). Used by the exoskeleton to speed up or slow down
K_t	A coefficient denoting the relation between q_T^d, $v_{H,d}$, and $y_1^a(x^-)$.
K_v	Coefficient denoting the relation between δv and q_T^a.
x_G	States corresponding to the global position and orientation (i.e. position and orientation relative to an inertial frame.)
x_H	States corresponding to Human subsystem (torso pitch angle and arm joint angles).
x_E	States corresponding to Exoskeleton subsystem
$\mathfrak{x}_H$	States corresponding to Human subsystem (torso pitch angle and arm joint angles) on the periodic orbit, $\mathcal{O}$, parametrized with the phase variable τ.
$\mathfrak{x}_E$	States corresponding to Exoskeleton subsystem (torso pitch angle and arm joint angles) on the periodic orbit, $\mathcal{O}$, parametrized with the phase variable τ.

Here, $T_i : \mathbb{R}^m \to \mathbb{R}^{n_i}$, is a constant matrix that selects the control input corresponding to the human or exoskeleton joints from the full dimensional input, $u_{IO,i}$, where n_i is the number of actuators corresponding the human or exoskeleton and $n_H + n_E = m$. $\mathcal{A}_i = [L_g y_{1,i}(\mathfrak{x}_i); L_g L_f y_{2,i}(\mathfrak{x}_i)]$ is the decoupling matrix corresponding to the human or the exoskeleton controller and μ_i is a linear feedback controller,

$$\mu_i = \begin{bmatrix} \mu_{1,i} \\ \mu_{2,i} \end{bmatrix} := \begin{bmatrix} -\bar{k}_i^p y_{1,i} \\ -2k_i^p y_{2,i} - k_i^d \dot{y}_{2,i} \end{bmatrix}, \tag{20}$$

for $k_i^p, \bar{k}_i^p, k_i^d$ diagonal matrices with positive entries. The control input for the full state is then given by the augmented control input, $u = [u_H; u_E]$.

In the decentralized control design presented above, it can be noticed that the exoskeleton controller does not have information about the true states of the human and vice versa. This is important since, in a practical setting, it may not be feasible to obtain measurements of human states. However, it is unclear if this controller will result in a stable system since we do not use full state information. Thus, Section VI covers numerical analysis using Poincaré maps to test stability and simulations to test robustness.

It is worth noting that the feedback linearizing control model for the human is not the only controller that can be applied to the human subsystem. In addition, other control designs have been tested, such as using joint level PD controllers on the human subsystem, which resulted in similar results. A feedback linearizing design has been chosen for the human subsystem to maintain consistency and similarity between the centralized controller and decentralized controller approaches. Further, it is assumed that the exoskeleton controller is robust enough that it would remain stable and capable of regulating velocity so long as the human is capable of maintaining a sufficiently decent tracking of their desired torso angle by the end of each step. Section VI will show results of the system being stable despite some steady state error in the human's torso tracking.

VI. RESULTS AND DISCUSSION

Numerical simulations are performed to investigate and compare the performance of the stabilizing controllers developed in the paper. In particular, the centralized and decentralized implementations of a controller for a fixed gait are first compared. The controllers are evaluated for their response to an initial condition that is not on the designed periodic orbit and for changes in the arm profiles adopted by the user. The point of the latter is that the user should not be constrained in how she moves her arms, while the optimization assumed the arms remain down and parallel to the body. Next, the centralized and decentralized implementations of speed regulation are compared over a varying speed profile. Finally, to test robustness of the proposed controller, the exoskeleton is simulated when walking up a ramp of a constant 5° slope. In all simulations, identical gains were used in the centralized and decentralized implementations of the controllers, and the same applies for walking on a flat surface versus a sloped surface.

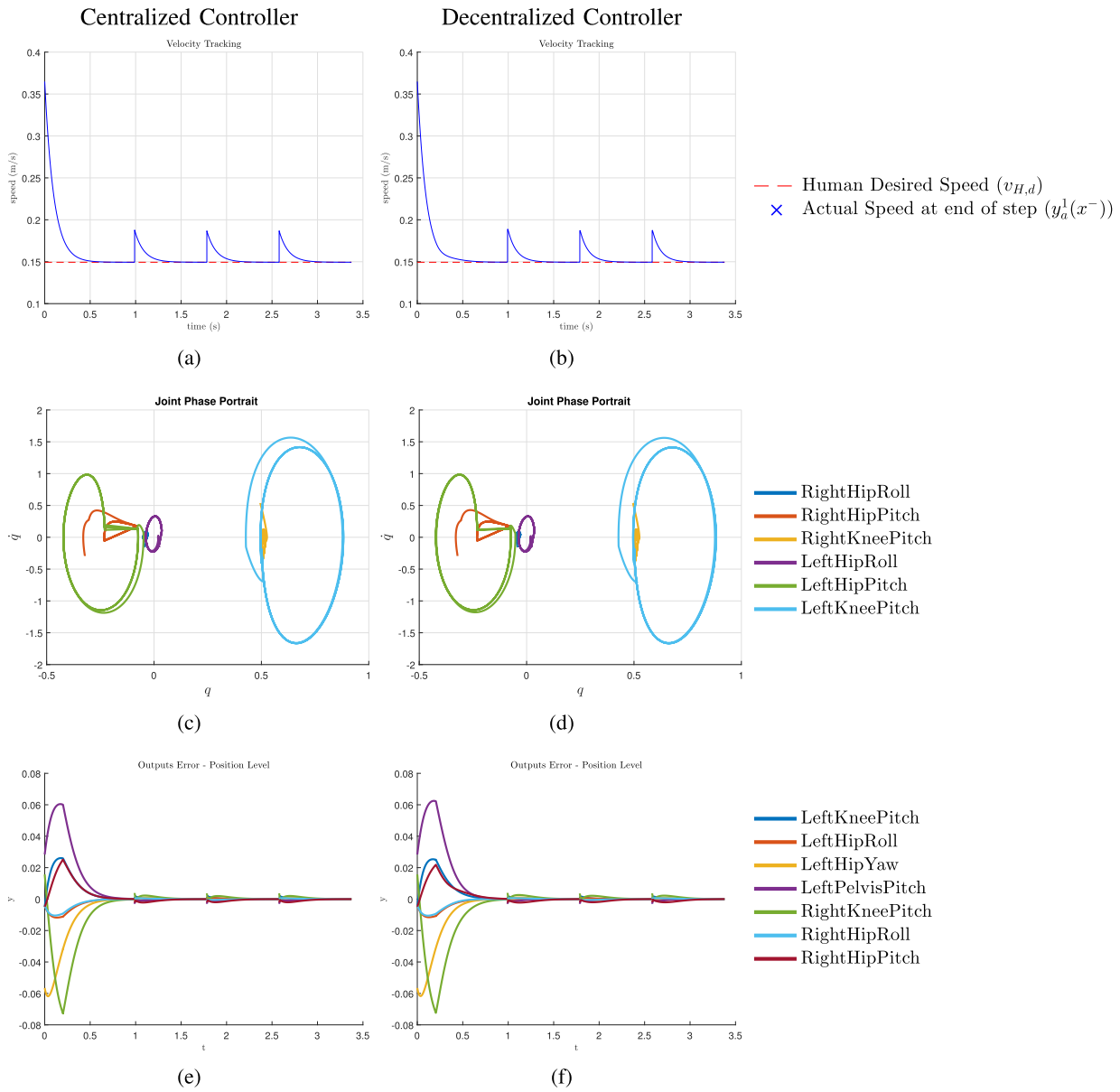

FIGURE 5. **Comparison between the Centralized and Decentralized controller in handling a perturbation in the initial conditions of the exoskeleton states; recall that the user has an upright posture. Both controllers are implementing the same periodic orbit. Figures a and b show the velocity tracking. Figures c and d show phase portraits converging to periodic orbits. Figures e and f show output errors converging to zero.**

A. CENTRALIZED VS DECENTRALIZED IMPLEMENTATIONS WITH A FIXED GAIT

In this first simulation, the user is not allowed to adjust the speed setpoint of the closed-loop system. The controller is operated with a fixed gait corresponding to $v_d = 0.15$ m/s, which is held constant step to step; moreover the user is assumed to maintain an erect torso, with the arms held fixed in the downward position. The purpose is to compare the centralized controller, that comes from the bipedal robotics literature, to its decentralized implementation, that respects the amount of shared information that can reasonably be expected between the user and the exoskeleton. The controllers are implemented as in Sect. V, with $q_T^d = 0\,^\circ$ and the output of the velocity library held constant.

To check the controllers' responses to off-orbit conditions, the initial condition of the exoskeleton is selected to be that of the periodic orbit of the gait for $v_d = 0.24$ m/s. Figures 5e and 5e shows both controllers driving the outputs nearly to zero before the end of each step. In addition, one can observe from the phase portraits in Fig. 5c and 5d that the periodic orbits of the closed-loop systems are indeed the same. In addition, it can be seen that both the centralized and decentralized controllers lead to a stable solution / behavior. We conjecture that their high similarity is because the

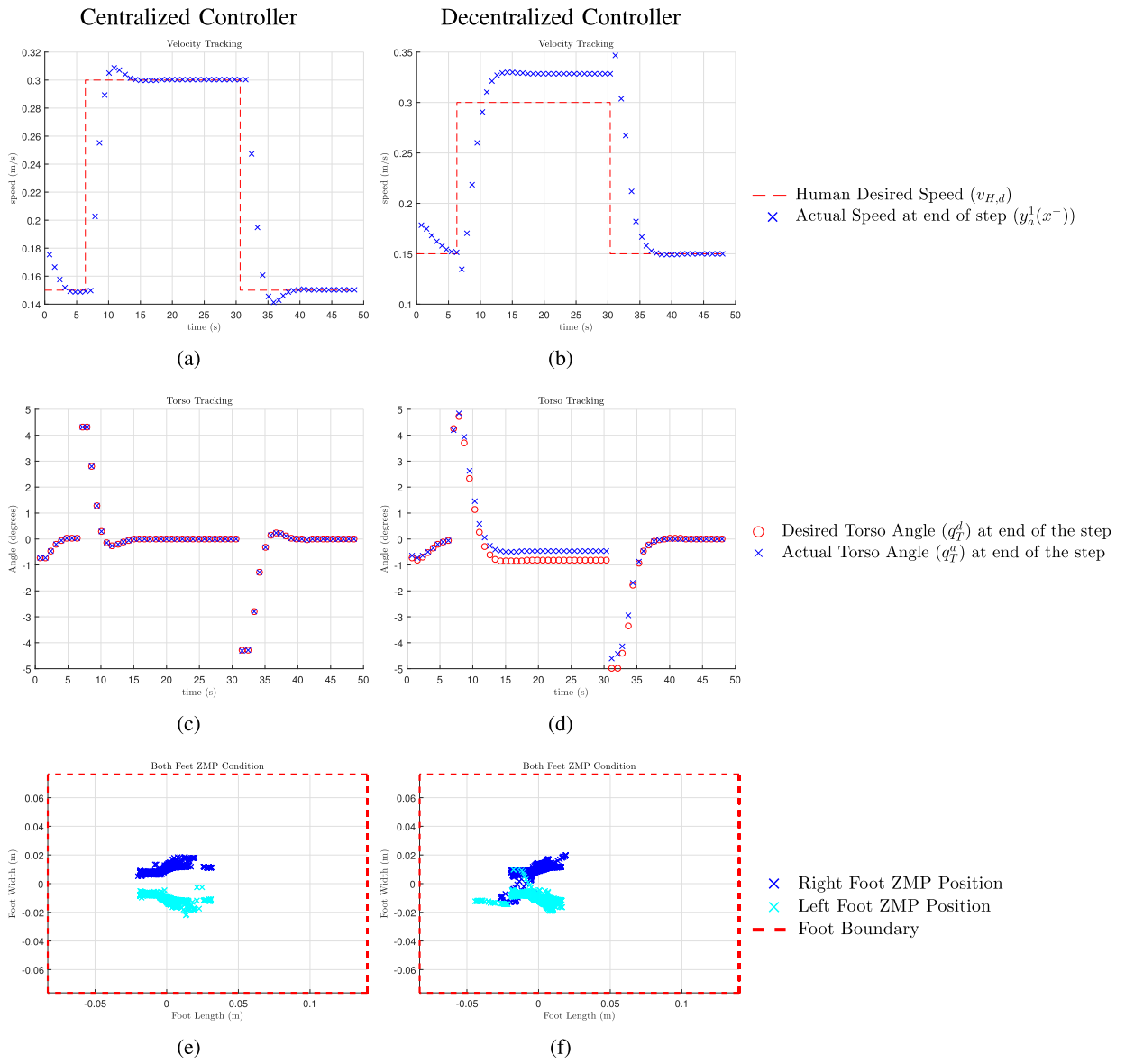

FIGURE 6. Comparison between Centralized and Decentralized controllers in tracking desired velocities. Figures a and b show the velocity tracking. Figures c and d torso tracking at the end of each step. Figures e and f show ZMP being within the foot's geometry.

perturbations are in the states of the exoskeleton. In addition, we conjecture that the upright posture of the user minimizes the effect of the user on the exoskeleton states.

B. CENTRALIZED VS DECENTRALIZED IMPLEMENTATIONS VELOCITY REGULATION

In this next set of simulations, the user is allowed to adjust the speed setpoint of the closed-loop system. The exoskeleton is walking on flat ground. In the first evaluation, the user's arms are controlled to a downward position, corresponding to the assumption of the gait design, and in the next simulation, they are swinging.

Figures 6a and 6b show both controllers responding to step changes in desired speed. The centralized and decentralized controllers each converge to a periodic steady state; phase portraits are shown in Fig. 6c and 6d. The steady-state speeds of the two controllers indicate that interpolated gaits are being employed. Figures 6e and 6f show that a key constraint, the ZMP, is being satisfied by the interpolated centralized and decentralized controllers. The other constraints, such as friction cone and torque bounds are also respected, though they are not shown here.

It is noted in Fig. 6a that the centralized controller achieves zero steady-state tracking error in the hip velocity, whereas in Fig. 6b, the decentralized controller sometimes has a non-zero steady-state error. A non-zero tracking error in the velocity occurs when the user's torso has a steady-state orientation error. In the highlighted section, the speed error of 0.028 m/s corresponds to a torso error of 0.36°. The steady-state error is of no practical importance because it could be removed

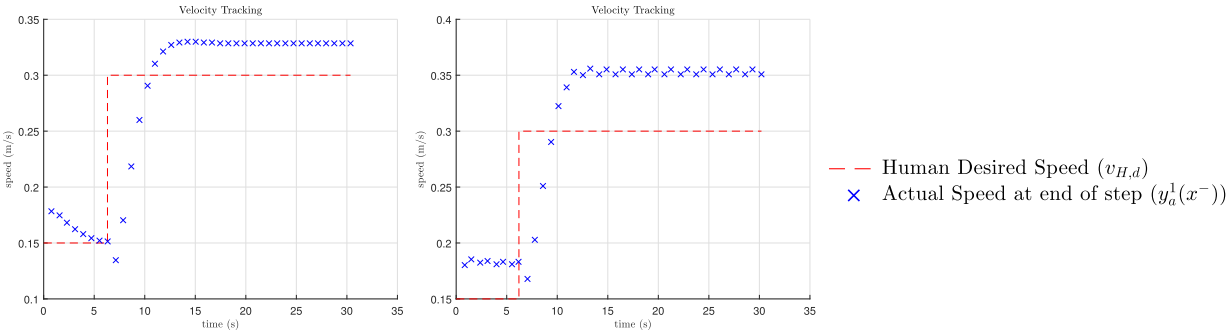

FIGURE 7. Comparison of the effect of arm swinging on the decentralized controller. Figure a shows the case with the arms stationary. Figure b shows the case with the arm swinging ±7.5ř. In both cases, the exoskeleton controller assumes that the arms are stationary.

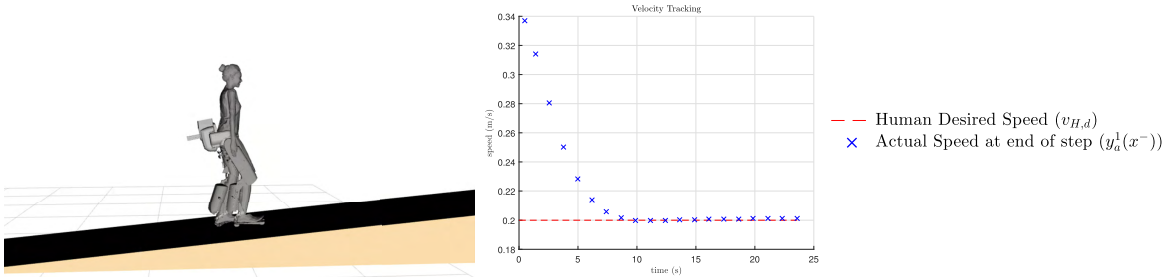

FIGURE 8. Simulation results of walking up a 5° slope. Figure a shows a snapshot of the simulation. Figure b shows the velocity tracking of the closed-loop system.

by augmenting the simple proportional controller proposed in (19) with an integral term, something the user would do through ''intuition'', or experience. More detail is given in Appendix IV.

C. EFFECTS OF ARM MOTION

Next, with the exoskeleton walking on level ground with the decentralized controller, the effects of the arms swinging ±7.5ř are evaluated; to be clear, the arm positions are unknown to the exoskeleton. The resulting velocity profiles are shown in Fig. 7a and 7b, where a period-2 oscillation is observed when the arms are swinging in Fig 7b. The amount of perturbation seems unlikely to be significant to a user. Though not shown, the action of the arms' motion has increased the steady-state error in the user's torso position. This does increase the steady-state error in the velocity. An experienced user would remove the torso error and cancel the velocity error as well.

D. WALKING UP A RAMP

Now, with the arms fixed downward and using the decentralized controller, the closed-loop system is challenged with a ramp of 5° incline.[2] The same library of gaits optimized for flat terrain are used here. The only change made is that it is assumed that the exoskeleton can sense ground slope for the purpose of orienting the swing foot parallel to the ground.

Figure 8b shows that the exoskeleton is indeed capable of walking up the slope without modifying the controller. In addition, the achieved velocity is close to the desired value.

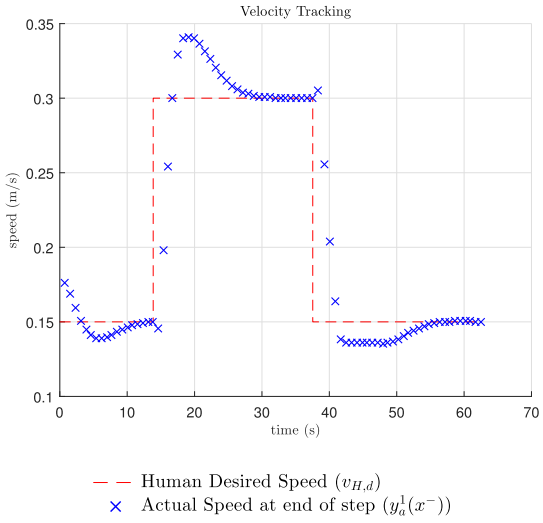

FIGURE 9. Simulated step response in the user's desired speed when an integral term is included in the model of the user's posture control.

[2]According to the 2010 ADA Guideline, ramps are considered part of an accessible route if their slope is no steeper than 1 : 12, with exceptions [6]. 5° is very close to the 4.8° recommended by the guidelines.

In addition, the simulation satisfies ZMP, friction cone, and torque bound constraints. Walking up the slope has resulted in the step duration increasing from approximately 0.8 s to 1.24 s.

VII. CONCLUSION

In this paper, we took recent tools from the design of control systems for bipedal robots and began their translation to an exoskeleton designed for patients with lower-limb paralysis. Drawing on methods based on virtual constraints, hybrid zero dynamics, and gait optimization, we developed a nonlinear decentralized control scheme for a lower-limb exoskeleton. In addition, a design for interfacing the human and the exoskeleton for velocity control is proposed. The overall controller is stabilizing, tracks the human's desired velocity, and is able to handle terrain variation, such as an upward slope. An important feature of the decentralized controller is that it does not require knowledge of the true state of the human, other than the torso angle, which is used to transmit desired velocity changes to the exoskeleton.

In future work, we intend to add additional degrees of freedom to the human model and allow the user to carry unmodeled loads, such as a backpack or a tablet in the user's hands. We will design a more complete set of gait primitives, including standing, walking faster, walking backwards, turning and sitting. We will also seek additional robustness to terrain variation using robust nonlinear controllers inspired by [12], [19], [30], and [31].

APPENDIX I
PARTIAL HYBRID ZERO DYNAMICS AND A CENTRAL CONTROLLER

With the aim of driving the outputs exponentially to zero, the control law,

$$u_{IO} := \mathcal{A}^{-1}\Big(\begin{bmatrix} 0 \\ L_f^2 y_2(q,\dot{q},\alpha,\beta)\end{bmatrix} + \begin{bmatrix} L_f y_1(q,\dot{q}) \\ k^d L_f y_2(q,\dot{q},\alpha,\beta)\end{bmatrix} + \begin{bmatrix} \bar{k}^p y_1(q,\dot{q},v_d) \\ 2k^p y_2(q,\alpha,\beta)\end{bmatrix}\Big), \tag{21}$$

where $k^p, \bar{k}^p, k^d$ are diagonal matrices with positive entries and the *Decoupling Matrix* $\mathcal{A}$ is given by

$$\mathcal{A} = \begin{bmatrix} L_g y_1(q,\dot{q}) \\ L_g L_f y_2(q,\dot{q},\alpha)\end{bmatrix}, \tag{22}$$

input-output linearizes the system and yields the exponentially stable linear output dynamics

$$\dot{y}_1 = -\bar{k}^p y_1, \tag{23}$$
$$\ddot{y}_2 = -2k^p y_2 - k^d \dot{y}_2. \tag{24}$$

Note that $L_f y_1$, $L_g y_1$, $L_f y_2$, $L_f^2 y_2$, and $L_g L_f y_2$ denote various Lie derivative of y_1, y_2 with respect to the vector fields f, g.

The input-output feedback controller, u_{IO}, renders the *zero dynamics* manifold, given by

$$\mathcal{Z} := \{x \in T\mathcal{Q} \mid y_1 = 0, y_2 = 0, L_f y_2 = 0\}, \tag{25}$$

invariant in the continuous dynamics, i.e., any solution that starts in $\mathcal{Z}$ remains in $\mathcal{Z}$ throughout the continuous phase. However, since the impact generally involves a jump on the velocity, the post impact velocity modulating output, y_1^+, is non zero, and consequently the zero dynamics manifold, $\mathcal{Z}$, is not impact variant under the choice of these outputs. Therefore, the hybrid invariance condition is enforced only on the position modulating outputs, resulting in the *Partial Zero Dynamics Surface* [7], defined as

$$\mathcal{PZ} := \{x \in T\mathcal{Q} \mid y_2 = 0, L_f y_2 = 0\}. \tag{26}$$

The Partial Zero Dynamics Surface is said to be impact invariant if the post impact states remain in $\mathcal{PZ}$, i.e.

$$\Delta(x) \in \mathcal{PZ}, \qquad \forall x \in S \cap \mathcal{PZ}. \tag{27}$$

The Partial Zero Dynamics Surface is hybrid invariant if it is invariant in the continuous dynamics and if it is impact invariant. If there exists a control input, u, for the system, Σ, such that $\mathcal{PZ}$ is hybrid invariant, then the system is said to have a *Partial Hybrid Zero Dynamics* (PHZD) surface. Moreover, by restricting the dynamics of the system on the PHZD surface, the analysis of periodic orbits for the full-order system can be done through those of the lower dimensional PHZD. Further details can be found in [8] and [27]. For the considered model and choice of outputs, these dynamics are of dimension 4 and described by the coordinates $(\tau, y_1, \dot{\tau}, \dot{y}_1)$. In the next section, we briefly summarize a gait generation technique, presented in [7], for determining the parameters α and v_d that define the desired outputs y_d.

APPENDIX II
GAIT GENERATION VIA DIRECT COLLOCATION METHOD

When using the HZD method of control design, the specification of stable walking gaits can be posed as a nonlinear constrained optimization problem. In other words, values for the desired output parameters, α and v_d, that satisfy invariance, periodicity and asymptotic stability constraints, can be determined while minimizing an objective function $\mathcal{J}(\mathbf{z})$, such as the cost of transport. In this paper, we use a *direct collocation* method to generate walking gaits for the human-exoskeleton system. Here, we only present a brief summary of the optimization problem and refer interested readers to [23] for a more detailed description.

We begin by representing the discretization of time by

$$0 = t_0 < t_1 < t_2 < \cdots < t_N = T_I, \tag{28}$$

where $T_I > 0$ is the time at which the system reaches a guard of the corresponding domain, $N = 2(N^c - 1)$, with $N^c \in \mathbb{Z}$ equal to the total number of even nodes, also called cardinal nodes. A key feature of this method is the introduction of defect variables. Determination of certain optimization variables in closed form may be computationally expensive in the optimization due to the relatively complicated nature of these functions. Defect variables avoid the explicit computation of

these variables by imposing implicit but equivalent equality constraints. The vector

$$z^i = (T_I^i, q^i, \dot{q}^i, \ddot{q}^i, u^i, F^i, \alpha^i, v_d^i, \beta^i) \tag{29}$$

is a set of optimization variables defined for each node, $i \in \{0, 1, 2, \ldots, N\}$. The direct collocation optimization is formulated as a nonlinear program (NLP),

$$z^* = \underset{z}{\text{argmin}}\ \mathcal{J}(z) \tag{30}$$

$$\text{s.t.} \quad z_{min} \leq z \leq z_{max}, \tag{31}$$

$$c_{min} \leq c(z) \leq c_{max}, \tag{32}$$

where $z = (\bar{\eta}^0, z^0, z^1, \ldots, z^N, \delta F^N)$ is a vector of decision variables, with $\bar{\eta}^0$ denoting the desired holonomic constraint at the first node, $c(z)$ is a vector of constraint functions, organized in the order of nodes and described in the next section, z_{min} and z_{max} are vectors containing the minimum and maximum values of the optimization variables respectively, and c_{min} and c_{max} are the vectors containing minimum and maximum values of constraints respectively, which are set to zero for equality constraints. Additionally, physical constraints, such as actuator input bounds, joint angle and velocity limits, can be incorporated as the boundary values of the corresponding optimization variable in z_{min} and z_{max}. The resulting direct collocation problem is solved by large sparse NLP solvers such as IPOPT [39], SNOPT [17], etc.

APPENDIX III
CONSTRAINTS FOR OPTIMIZATION

The following constraints are enforced for the optimization and determine the functions $c(z)$ in (32):

(a) *Defect Constraints*: These are constraints on the estimated states from the optimizer and states obtained from the interpolation polynomial. A complete description of defect constraints can be found in [23].
(b) *System and linear output dynamics*: The system dynamics, (1) and (2), and the closed-loop linear output dynamics, (23) and (24) are imposed as equality constraints.
(c) *PHZD Condition*: The relative degree two outputs must be zero at the beginning of each domain, i.e., the condition in (27) must be satisfied.
(d) *Periodicity of an orbit*: Post impact states at the last node at the current domain must be equal to the first node of the next domain.
(e) *Parameter consistency*: The parameters, $(\alpha^i, \beta^i, v_d^i)$ and the time T_I^i, at each time step, i, need to be consistent and constant throughout and between each domain.
(f) *Domain of admissibility*: The domain of admissibility constraints, (5), must be satisfied to ensure holonomic and unilateral constraints are met.
(g) *Guard condition*: To ensure that the system reaches the appropriate guard condition, the conditions in (6) are imposed on the last node.
(h) *Holonomic constraints*: (3) and (2), ensure that the holonomic constraints are held constant. However, to ensure that they are held at the correct constant, additional set of constraints are required that explicitly enforce this, i.e. the constraint, $\eta - \bar{\eta}^0 = 0$, is enforced at the first node of each domain.
(i) *Time parameterization*: According to (12), the parameters β_1 and β_2 represent the linearized hip position in the sagittal plane, δp_{hip} at the beginning and at the end of a gait respectively. These conditions must be enforced at the first and the last node of each domain, respectively.
(j) *Walking Speed, Step Length and Foot clearance*: A desired forward walking speed, step length and swing foot clearance may be provided to achieve the required walking behavior.
(k) *Foot retraction*: The forward velocity of the swing foot before impact must be negative. This reduces impact loses and, when combined with the foot clearance constraint, helps avoid cases of gaits with foot scuffing.
(l) *Rigid human*: The human subsystem is constrained to have torso and arm angles fixed, with the torso upright relative to the exoskeleton and the arms fixed downwards.

APPENDIX VI
EVENT-BASED INTEGRAL COMPONENT IN HUMAN TORSO CONTROLLER

While a steady-state error was observed in Sec. VI-B, it is conjectured that a user will naturally compensate for the error using what resembles an integral controller. To support this idea, the controller law from 19 is augmented by a simple discrete-time integral term to show how one remove the steady-state error. Similar control design has been developed for bipeds to track walking speeds [40]. Let the new model of a human's control system be

$$q_T^d := K_t * (v_{H,d} - y_1^a(x^-)) + K_{tI} * v_{err,intg}^i,$$
$$v_{err,intg}^i := v_{err,intg}^{i-1} + (v_{H,d} - y_1^a(x^-)),$$

where K_{tI} is the integral gain of the controller and $v_{err,intg}^i$ is the discrete-time (or event-based) integration of the velocity error at the i^{th} step. All other parameters are as defined in 19. The gains used are $K_{ti} = 0.065$. In addition, $v_{err,intg}^i$ is saturated at ± 0.2. All other gains are kept the same as in Sec. VI-B.

Figure 9 shows the result of running a simulation with the updated controller. As expected, the actual velocity converges to the desired velocity. With a pre-filter, the overshoot could be removed, but once again, we believe a user would quickly master this skill.

Acknowledgment

(Ayush Agrawal and Omar Harib contributed equally to this work.)

REFERENCES

[1] *130 Rehabilitation Centers Worldwide*, accessed on Dec. 7, 2016. [Online]. Available: http://eksobionics.com/
[2] *Cybathlon Championship for Athletes With Disabilities | ETH Zurich*, accessed on Dec. 7, 2016. [Online]. Available: http://www.cybathlon.ethz.ch/en/
[3] *Rewalk 6.0—Home*, accessed on Dec. 7, 2016. [Online]. Available: http://rewalk.com/

[4] *Step into the Future*, accessed on Dec. 7, 2016. [Online]. Available: http://www.rexbionics.com/

[5] *Wandercraft*, accessed on Dec. 7, 2016. [Online]. Available: http://www.wandercraft.eu/

[6] (Sep. 2010). *2010 ADA Standards for Accessible Design*. [Online]. Available: https://www.ada.gov/regs2010/2010ADAStandards/2010ADAStandards.pdf

[7] A. D. Ames, "Human-inspired control of bipedal walking robots," *IEEE Trans. Autom. Control*, vol. 59, no. 5, pp. 1115–1130, May 2014.

[8] A. D. Ames, E. A. Cousineau, and M. J. Powell, "Dynamically stable bipedal robotic walking with NAO via human-inspired hybrid zero dynamics," in *Proc. 15th ACM Int. Conf. Hybrid Syst., Comput. Control*, 2012, pp. 135–144.

[9] B. Chen *et al.*, "Design of a lower extremity exoskeleton for motion assistance in paralyzed individuals," in *Proc. IEEE Int. Conf. Robot. Biomimetics (ROBIO)*, Dec. 2015, pp. 144–149.

[10] E. Cousineau and A. D. Ames, "Realizing underactuated bipedal walking with torque controllers via the ideal model resolved motion method," in *Proc. IEEE Int. Conf. Robot. Autom. (ICRA)*, May 2015, pp. 5747–5753.

[11] X. Da, O. Harib, R. Hartley, B. Griffin, and J. W. Grizzle, "From 2D design of underactuated bipedal gaits to 3D implementation: Walking with speed tracking," *IEEE Access*, vol. 4, pp. 3469–3478, 2016.

[12] X. Da, R. Hartley, and J. W. Grizzle, "First steps toward supervised learning for underactuated bipedal robot locomotion, with outdoor experiments on the wave field," in *Proc. Int. Conf. Robot. Automat. (ICRA)*, 2017, pp. 1–8. [Online]. Available: http://web.eecs.umich.edu/faculty/grizzle/papers/XingyeDa_ICRA2017.pdf

[13] A. M. Dollar and H. Herr, "Lower extremity exoskeletons and active orthoses: Challenges and state-of-the-art," *IEEE Trans. Robot.*, vol. 24, no. 1, pp. 144–158, Feb. 2008.

[14] A. Esquenazi, M. Talaty, A. Packel, and M. Saulino, "The ReWalk powered exoskeleton to restore ambulatory function to individuals with thoracic-level motor-complete spinal cord injury," *Amer. J. Phys. Med. Rehabil.*, vol. 91, no. 11, pp. 911–921, 2012.

[15] M. Fontana, R. Vertechy, S. Marcheschi, F. Salsedo, and M. Bergamasco, "The body extender: A full-body exoskeleton for the transport and handling of heavy loads," *IEEE Robot. Autom. Mag.*, vol. 21, no. 4, pp. 34–44, Dec. 2014.

[16] K. Galloway, K. Sreenath, A. D. Ames, and J. W. Grizzle, "Torque saturation in bipedal robotic walking through control Lyapunov function-based quadratic programs," *IEEE Access*, vol. 3, pp. 323–332, 2015.

[17] P. E. Gill, W. Murray, and M. A. Saunders, "SNOPT: An SQP algorithm for large-scale constrained optimization," *SIAM Rev.*, vol. 47, no. 1, pp. 99–131, 2005.

[18] R. D. Gregg, T. Lenzi, L. J. Hargrove, and J. W. Sensinger, "Virtual constraint control of a powered prosthetic leg: From simulation to experiments with transfemoral amputees," *IEEE Trans. Robot.*, vol. 30, no. 6, pp. 1455–1471, Dec. 2014.

[19] B. Griffin and J. Grizzle, "Walking gait optimization for accommodation of unknown terrain height variations," in *Proc. Amer. Control Conf.*, Jul. 2015, pp. 4810–4817.

[20] J. W. Grizzle, C. Chevallereau, A. D. Ames, and R. W. Sinnet, "3D bipedal robotic walking: Models, feedback control, and open problems," *IFAC Proc. Vol.*, vol. 43, no. 14, pp. 505–532, Sep. 2010.

[21] J. G. Grundmann and A. Seireg, "Computer control of multi-task exoskeleton for paraplegics," in *Proc. 2nd CISM/IFTOMM Int. Symp. Theory Pract. Robots Manipulators*, 1977, pp. 233–240.

[22] K. A. Hamed and R. D. Gregg, "Decentralized feedback controllers for exponential stabilization of hybrid periodic orbits: Application to robotic walking," in *Proc. Amer. Control Conf.*, Boston, MA, USA, Jul. 2016, pp. 4793–4800.

[23] A. Hereid, E. A. Cousineau, C. M. Hubicki, and A. D. Ames, "3D dynamic walking with underactuated humanoid robots: A direct collocation framework for optimizing hybrid zero dynamics," in *Proc. IEEE Int. Conf. Robot. Autom.*, May 2016, pp. 1447–1454.

[24] D. Hristic, M. Vukobratovic, and M. Timotijevic, "New model of autonomous 'active suit' for distrophic patients," in *Proc. Int. Symp. External Control Human Extremities*, 1981, pp. 33–42.

[25] Y. Hurmuzlu, F. Génot, and B. Brogliato, "Modeling, stability and control of biped robots—A general framework," *Automatica*, vol. 40, no. 10, pp. 1647–1664, Oct. 2004.

[26] P. Malcolm, W. Derave, S. Galle, and D. De Clercq, "A simple exoskeleton that assists plantarflexion can reduce the metabolic cost of human walking," *PLoS ONE*, vol. 8, no. 2, p. e56137, Jan. 2013.

[27] B. Morris and J. W. Grizzle, "Hybrid invariant manifolds in systems with impulse effects with application to periodic locomotion in bipedal robots," *IEEE Trans. Autom. Control*, vol. 54, no. 8, pp. 1751–1764, Aug. 2009.

[28] R. M. Murray, Z. Li, S. S. Sastry, and S. S. Sastry, *A Mathematical Introduction to Robotic Manipulation*. Boca Raton, FL, USA: CRC Press, 1994.

[29] P. D. Neuhaus, J. H. Noorden, T. J. Craig, T. Torres, J. Kirschbaum, and J. E. Pratt, "Design and evaluation of Mina: A robotic orthosis for paraplegics," in *Proc. IEEE Int. Conf. Rehabil. Robot.*, Jun./Jul. 2011, pp. 1–8.

[30] Q. Nguyen and K. Sreenath, "Optimal robust control for constrained nonlinear hybrid systems with application to bipedal locomotion," in *Proc. Amer. Control Conf. (ACC)*, Jul. 2016, pp. 4807–4813.

[31] Q. Nguyen and K. Sreenath, "Optimal robust control for bipedal robots through control Lyapunov function based quadratic programs," in *Proc. Robot., Sci. Syst.*, Rome, Italy, 2015, pp. 1–9.

[32] A. Ramezani, J. W. Hurst, K. A. Hamed, and J. W. Grizzle, "Performance analysis and feedback control of ATRIAS, a three-dimensional bipedal robot," *ASME J. Dyn. Syst., Meas., Control*, vol. 136, no. 2, p. 021012, Dec. 2013.

[33] Y. Sankai, *HAL: Hybrid Assistive Limb Based on Cybernics*, vol. 66. Berlin, Germany: Springer, 2011, pp. 25–34.

[34] A. Seireg and J. G. Grundmann, "Design of a multitask exoskeletal walking device for paraplegics," *Biomechan. Med. Devices*, pp. 569–644, 1981.

[35] J. Sensinger, "Prostheses and exoskeletons: Moving from a mechatronics bottleneck through a controls bottleneck," in *Proc. 3rd Int. Conf. Control, Dyn. Syst., Robot.*, May 2016, pp. 1–2.

[36] K. Sreenath, H.-W. Park, I. Poulakakis, and J. W. Grizzle, "A compliant hybrid zero dynamics controller for stable, efficient and fast bipedal walking on MABEL," *Int. J. Robot. Res.*, vol. 30, no. 9, pp. 1170–1193, Sep. 2010.

[37] T. A. Swift, "Control and trajectory generation of a wearable mobility exoskeleton for spinal cord injury patients," Ph.D. dissertation, Dept. Mech. Eng., Univ. California, Berkeley, Berkeley, 2011.

[38] M. Vukobratovic, D. Hristic, and Z. Stojiljkovic, "Development of active anthropomorphic exoskeletons," *Med. Biol. Eng.*, vol. 12, no. 1, pp. 66–80, Jan. 1974.

[39] A. Wächter and L. T. Biegler, "On the implementation of an interior-point filter line-search algorithm for large-scale nonlinear programming," *Math. Program.*, vol. 106, no. 1, pp. 25–57, Mar. 2006.

[40] E. R. Westervelt, J. W. Grizzle, and C. C. de Wit, "Switching and PI control of walking motions of planar biped walkers," *IEEE Trans. Autom. Control*, vol. 48, no. 2, pp. 308–312, Feb. 2003.

[41] E. R. Westervelt, J. W. Grizzle, C. Chevallereau, J. H. Choi, and B. Morris, *Feedback Control of Dynamic Bipedal Robot Locomotion*, vol. 28. Boca Raton, FL, USA: CRC Press, 2007.

[42] K. Yamamoto, K. Hyodo, M. Ishii, and T. Matsuo, "Development of power assisting suit for assisting nurse labor," *JSME Int. J. Ser. C*, vol. 45, no. 3, pp. 703–711, 2002.

[43] J. Yao, Z. Jiao, and D. Ma, "Adaptive robust control of DC motors with extended state observer," *IEEE Trans. Ind. Electron.*, vol. 61, no. 7, pp. 3630–3637, Jul. 2014.

[44] H. Zhao, S. Kolathaya, and A. D. Ames, "Quadratic programming and impedance control for transfemoral prosthesis," in *Proc. IEEE Int. Conf. Robot. Autom.*, May/Jun. 2014, pp. 1341–1347.

[45] H. Zhao, J. Horn, J. Reher, V. Paredes, and A. D. Ames, "First steps toward translating robotic walking to prostheses: A nonlinear optimization based control approach," *Auto. Robots*, vol. 41, no. 3, pp. 725–742, Mar. 2016.

[46] A. B. Zoss, H. Kazerooni, and A. Chu, "Biomechanical design of the Berkeley lower extremity exoskeleton (BLEEX)," *IEEE/ASME Trans. Mechatronics*, vol. 11, no. 2, pp. 128–138, Apr. 2006.

AYUSH AGRAWAL received the B.Tech. degree in mechanical engineering from the National Institute of Technology, Karnataka, India, in 2015. He is currently pursuing the M.Sc. degree with the Department of Mechanical Engineering, Carnegie Mellon University, Pittsburgh, PA, under the supervision of K. Sreenath with the Hybrid Dynamic Robotics Laboratory. His research interests are in the areas of nonlinear control and bipedal locomotion.

OMAR HARIB was double majored and received the bachelor's degrees in mechanical engineering and computer engineering from the American University of Sharjah, UAE. He is currently pursuing the Ph.D. degree in electrical and computer engineering from the University of Michigan, Ann Arbor. His current research interests are in control theory and experimentation focusing on bipedal robot locomotion.

AYONGA HEREID received the Ph.D. degree in mechanical engineering from the Georgia Institute of Technology in 2016. He is currently a Post-Doctoral Research Fellow with the Department of Electrical Engineering and Computer Science, University of Michigan. His current research interests center around developing advanced nonlinear optimization and control algorithms to realize dynamic and natural locomotion on bipedal robots. He received the DENSO Best Student Paper Award of the 17th International Conference on Hybrid System: Computation and Control in 2014.

SYLVAIN FINET received the degree from ENSTA Paristech in 2013. He is currently pursuing the Ph.D. degree in bipedal locomotion with Mines ParisTech. He is also a Control Command Engineer with Wandercraft. His current research interests are both the theoretical and experimental aspects of nonlinear control and bipedal locomotion.

MATTHIEU MASSELIN received the degree and the M.Sc. degree in electro-physics from Ecole Polytechique and Kungliga Tekniska Högskolan, Stockholm in 2013. He joined Wandercraft after where he has been developing the control team. He has lead an effort to implement dynamic walking on Wandercraft exoskeleton, building on knowledge developed for biped robots.

LAURENT PRALY received the M.S. degree in engineering from the École Nationale Supérieure des Mines de Paris, Paris, France, in 1976, and the Ph.D. degree in automatic control and mathematics from the Université Paris IX Dauphine, Paris, France, in 1988. Since 1980, he has been with the Centre Automatique et Systèmes, École des Mines de Paris. His main interest is in observers and feedback stabilization/regulation for controlled dynamical systems under various aspects, linear and nonlinear, dynamic, output, under constraints, with parametric or dynamic uncertainty, disturbance attenuation or rejection. On these topics, he is contributing both on the theoretical aspect with many academic publications and the practical aspect with applications in power systems, electric drives, mechanical systems, aerodynamical, and space vehicles.

AARON D. AMES received the B.S. degree in mechanical engineering and the B.A. degree in mathematics from the University of St. Thomas in 2001, and the M.A. degree in mathematics and the Ph.D. degree in electrical engineering and computer sciences from the University of California at Berkeley, Berkeley, in 2006. He was an Associate Professor with the Woodruff School of Mechanical Engineering and the School of Electrical & Computer Engineering, Georgia Institute of Technology. He served as a Post-Doctoral Scholar in control and dynamical systems with California Institute of Technology, from 2006 to 2008, and a Faculty with Texas A&M University in 2008. In 2017, he joined California Institute of Technology, where he is currently the Bren Professor of Mechanical and Civil Engineering and Control and Dynamical Systems. His research interests span the areas of robotics, nonlinear control, and hybrid systems, with a special focus on applications to bipedal robotic walking—both formally and through experimental validation. His laboratory designs, builds and tests novel bipedal robots, humanoids, and prostheses with the goal of achieving human-like bipedal robotic locomotion and translating these capabilities to robotic assistive devices. At UC Berkeley, he was a recipient of the 2005 Leon O. Chua Award for achievement in nonlinear science and the 2006 Bernard Friedman Memorial Prize in Applied Mathematics. He received the NSF CAREER Award in 2010 and the 2015 Donald P. Eckman Award.

KOUSHIL SREENATH received the Ph.D. degree in electrical engineering: systems and the M.S. degree in applied mathematics from the University of Michigan, Ann Arbor, MI, in 2011. He is currently an Assistant Professor of Mechanical Engineering, Robotics Institute, and Electrical & Computer Engineering, Carnegie Mellon University. His research interest lies at the intersection of highly dynamic robotics and applied nonlinear control. He received the Best Paper Award in RSS 2013 and the Google Faculty Research Award in Robotics in 2015.

JESSY W. GRIZZLE (S'78–M'83–F'97) received the Ph.D. degree in electrical engineering from The University of Texas at Austin in 1983. He is currently a Professor of Electrical Engineering and Computer Science with the University of Michigan, where he holds the titles of the Elmer Gilbert Distinguished University Professor and the Jerry and Carol Levin Professor of Engineering. He jointly holds sixteen patents dealing with emissions reduction in passenger vehicles through improved control system design. He is a fellow of the IFAC. He received the Paper of the Year Award from the IEEE Vehicular Technology Society in 1993, the George S. Axelby Award in 2002, the Control Systems Technology Award in 2003, the Bode Prize in 2012, and the IEEE TRANSACTIONS ON CONTROL SYSTEMS TECHNOLOGY Outstanding Paper Award in 2014. His work on bipedal locomotion has been the object of numerous plenary lectures and has been featured on CNN, ESPN, Discovery Channel, The Economist, Wired Magazine, Discover Magazine, Scientific American, and Popular Mechanics.